Electrodisintegration of ^{56}Fe, ^{59}Co, and ^{64}Zn

W. R. Dodge, R. G. Leicht,* E. Hayward, and E. Wolynec†
National Bureau of Standards, Washington, D. C. 20234
(Received 21 May 1981)

The (e,p) and (e,α) cross sections for ^{56}Fe, ^{59}Co, and ^{64}Zn have been measured in the electron energy range 16–100 MeV. They have been analyzed using the distorted-wave Born approximation $E1$ and $E2$ virtual photon spectra. The $E1$ and $E2$ components in the proton and α channels have been obtained.

[NUCLEAR REACTIONS ^{56}Fe(e,p), ^{56}Fe(e,α), ^{59}Co(e,p), ^{59}Co(e,α), ^{64}Zn(e,p), and ^{64}Zn(e,α); measured $\sigma(E_0,E_x,34°)$, $\sigma(E_0,E_x,48°)$, $\sigma(E_0,E_x,62°)$, $\sigma(E_0,E_x,90°)$, $\sigma(E_0,E_x,118°)$, $\sigma(E_0,E_x,132°)$; obtained $\sigma(e,p)$, $\sigma(e,\alpha)$; deduced $\sigma^{E1}_{\gamma,p}(E)$, $\sigma^{E2}_{\gamma,p}(E)$, $\sigma^{E1}_{\gamma,\alpha}(E)$, $\sigma^{E2}_{\gamma,\alpha}(E)$.]

I. INTRODUCTION

In a previous work[1] we described an experiment in which the (e,p) and (e,α) cross sections for three nickel isotopes were studied. The present paper describes an extension of that work to include three new targets: ^{56}Fe, ^{59}Co, and ^{64}Zn. These targets were chosen because their Coulomb barriers are low enough to allow α-particle emission from the isoscalar $E2$ resonance. ^{56}Fe is a common target and we hoped to make comparisons with other work. We chose ^{59}Co to see if there were any striking differences for an odd-A nucleus and ^{64}Zn because its α-particle and proton yields are very large owing to low binding energies. The various separation energies are listed in Table I. A preliminary report[2] of some of these results has already been given.

TABLE I. Separation energies and target properties.

Target	^{56}Fe	^{59}Co	^{64}Zn
$S(N)$ (MeV)	11.2	10.5	11.9
$S(P)$ (MeV)	10.2	7.36	7.71
$S(\alpha)$ (MeV)	7.61	6.94	3.96
$S(2N)$ (MeV)	20.5	19.0	21.0
$S(2P)$ (MeV)	18.3	19.3	13.8
$S(P\alpha)$ (MeV)	18.1	15.0	13.5
Enrichment (%)	99.93		99.85
Thickness (mg/cm^2)	1.48	1.59	1.51

II. THE EXPERIMENT

The present experiment was performed in much greater detail than the previous one.[1] The doubly differential cross sections, $d^2\sigma/d\Omega\, dT$ for the electroproduction of protons and α particles from these targets, were measured as a function of incident electron energy from 16 to 100 MeV, using a magnetic spectrometer having circular solid state detectors in its focal plane. Complete energy spectra were measured at 90° for electron energies of 16, 18, 20, 22.5, 27.5, 30, and 50 MeV and at 34°, 48°, 90°, and 132° for 50 MeV incident electrons. Table I gives the target thicknesses and enrichment.

The spectra, examples of which are shown in Figs. 1 and 2, are typical evaporation spectra peaking near 5 MeV for the protons and near 8 MeV for the α particles and having an asymmetry characteristic of Coulomb barrier penetration. Above 30 MeV the shapes of the spectra are independent of the bombarding energy except for the high energy tail,[3,4] the magnitude and extent of which increases with the electron energy.

Several bumps or structures were observed in the proton spectra when the incident electron energies were below ~25 MeV. These are evident in Fig. 1 and become more pronounced as the incident electron energy is decreased. In Table II are listed the peaks that are apparent in several of the spectra generated by low energy electrons. These protons populate states near the ground state in the residual nuclei. Similar structures were also reported in Ref. 5.

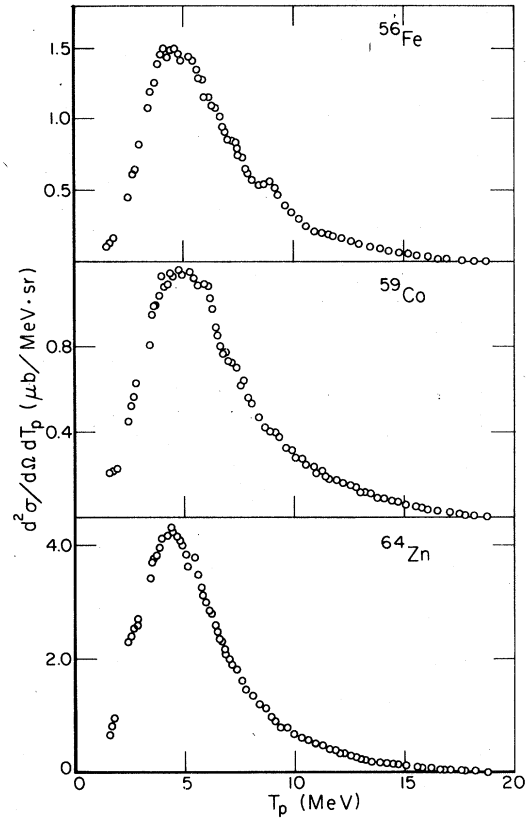

FIG. 1. The proton spectra produced at 90° when 30 MeV electrons are incident on targets of ^{56}Fe, ^{59}Co, and ^{64}Zn.

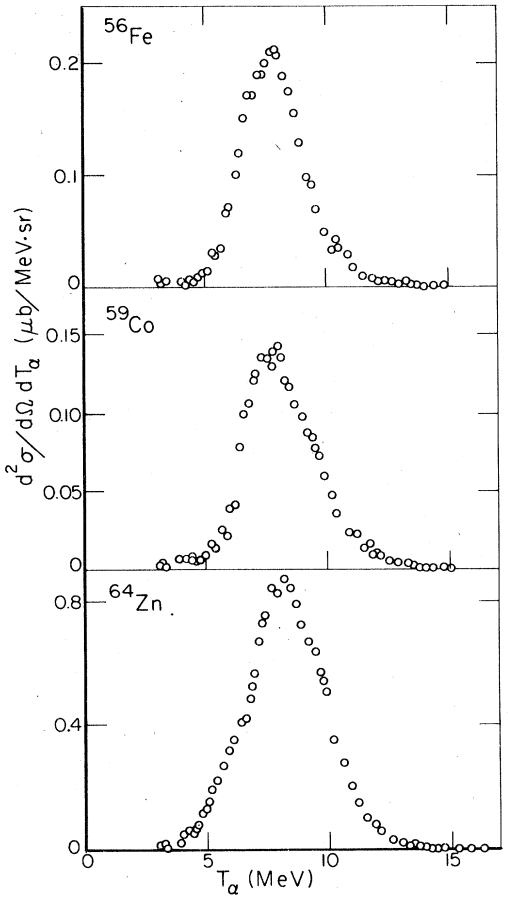

FIG. 2. The α-particle spectra produced at 90° when 30 MeV electrons are incident on targets of ^{56}Fe, ^{59}Co, and ^{64}Zn.

In order to obtain the differential cross sections $d\sigma/d\Omega(90°)$, the yield curves for protons and α particles in two energy intervals near the peaks of the energy spectra, 4.38—4.95 and 7.54—8.46 MeV, were measured at 90° for many incident electron energies extending as far as 100 MeV. From the complete energy spectra the ratio of the total number of particles to the number in the energy interval was obtained. An interpolation and extrapolation of these ratios allowed us to integrate over the outgoing particle energy, T_p or T_α, to obtain the cross section $d\sigma/d\Omega(90°)$. Since the measurements made at the other angles indicated that $d\sigma/d\Omega$ is very nearly independent of the angle, the total cross sections $\sigma_{e,p}(E_0)$ and $\sigma_{e,\alpha}(E_0)$ were obtained by multiplying the 90° cross section by 4π; the error introduced by this approximation is $\sim 2-3\%$.

In the range of incident electron energy 36—100 MeV, the 90°-yield curves were also measured with a radiator interposed 7.6 cm ahead of the target but out of view of the spectrometer. The electrons multiple scatter in the 217 mg/cm^2 tantalum radiator enlarging the beam spot size on the target and altering the effective momentum acceptance interval of the spectrometer because the focal plane detectors are circular rather than rectangular. A correction for this effect, described in Ref. 1, has been made which increases the yields by about 10% at 36 MeV, 5% at 50 MeV, and becomes negligible at 70 MeV.

TABLE II. Energies of observed proton groups.

Nucleus	Proton energy (MeV)
^{56}Fe	7.1
	9
^{59}Co	6.3
^{64}Zn	5.5

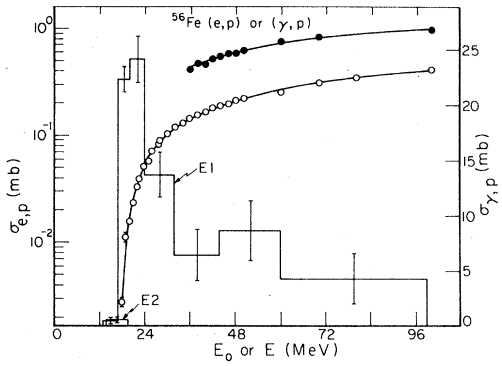

FIG. 3. The measured $\sigma_{e,p}(E_0)$ for ^{56}Fe as a function of total incident electron energy E_0 (open circles). The full circles represent the yield $Y_{e,p}(E_0)$ obtained when a 0.217 g/cm^2 tantalum foil was placed in the electron beam ahead of the target. The smooth curves are the best fits to the data and were obtained by combining the histograms representing the $E1$ and $E2$ (γ,p) cross sections (right-hand scale) in Eqs. (1) and (2) with the $E1$ and $E2$ DWBA virtual photon spectra and by making use of the DBM bremsstrahlung cross section. The size effect correction described in the text has been applied to the virtual photon spectra.

Since the shapes of the particle spectra obtained with the radiator in were not significantly different from those measured with the radiator out, the yields of electrodisintegration plus photodisintegration, $Y_{e,p}(E_0)$ and $Y_{e,\alpha}(E_0)$, with the radiator in were obtained by multiplying by the same factors used to obtain the cross sections $\sigma_{e,p}(E_0)$ and $\sigma_{e,\alpha}(E_0)$. The cross sections and yields for each of the six reactions studied are shown in Figs. 3—8. The data of Skopik, Asai, and Murphy,[6] who measured the ^{56}Fe(e,α) cross section, are included in Fig. 6 to illustrate the good agreement between the two experiments.

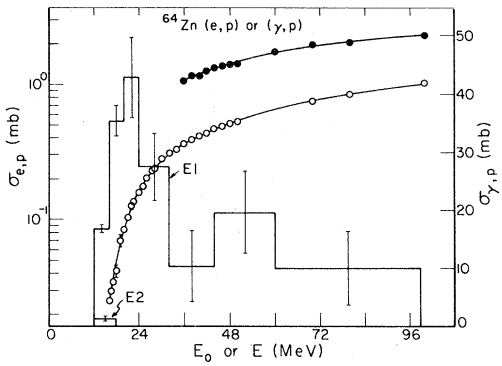

FIG. 5. The $\sigma_{e,p}(E_0)$ for ^{64}Zn. See caption of Fig. 3.

III. DATA ANALYSIS

The electrodisintegration cross section $\sigma_{e,x}(E_0)$ may be obtained from the photonuclear cross section $\sigma_{\gamma,x}^{\lambda L}(E)$ through an integral over the virtual photon intensity spectrum $N^{\lambda L}(E_0,E,Z)$:

$$\sigma_{e,x}(E_0)=\int_0^{E_0-m}\sum_{\lambda L}\sigma_{\gamma,x}^{\lambda L}(E)N^{\lambda L}(E_0,E,Z)\frac{dE}{E}. \quad (1)$$

In Eq. (1), E_0 stands for the total electron energy and E stands for the excitation energy of multipolarity λL. In the same spirit the yield with the radiator in is

$$Y_{e,x}(E_0)=\sigma_{e,x}(E_0-2\Delta E_0)+N_r\int_0^{E_0-m}\sum_{\lambda L}\sigma_{\gamma,x}^{\lambda L}(E)K(E_0-\Delta E_0,E)\frac{dE}{E}, \quad (2)$$

where N_r is the number of nuclei/cm^2 in the tantalum radiator, $K(E_0,E)$ is the bremsstrahlung cross section in tantalum, and ΔE_0 is the electron energy loss in half the radiator thickness.

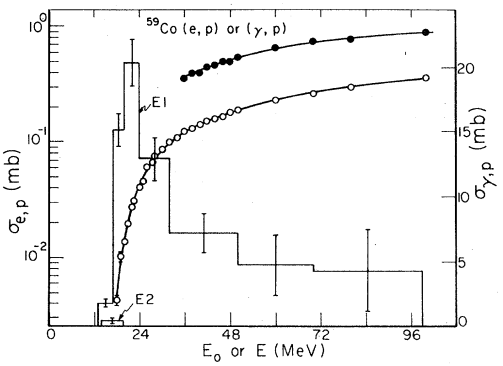

FIG. 4. The $\sigma_{e,p}(E_0)$ for ^{59}Co. See caption of Fig. 3.

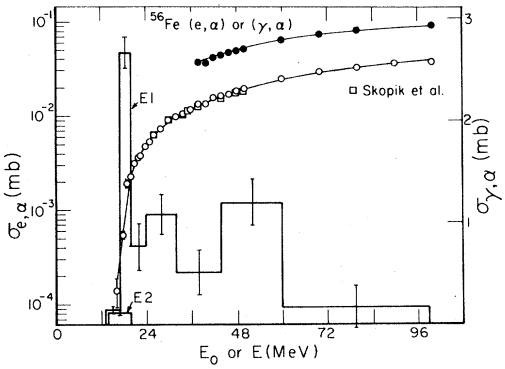

FIG. 6. The $\sigma_{e,\alpha}(E_0)$ for ^{56}Fe. See caption of Fig. 3. The squares represent the data of Ref. 6 and are included to show the good agreement between the two experiments.

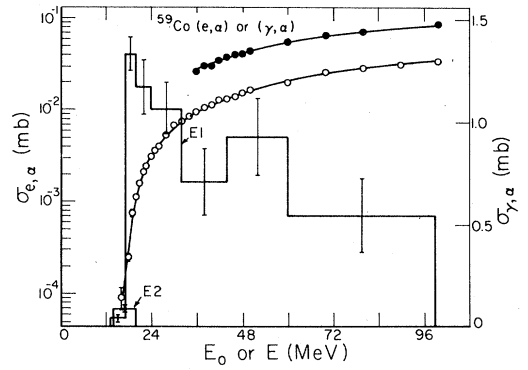

FIG. 7. The $\sigma_{e,\alpha}(E_0)$ for ^{59}Co. See caption of Fig. 3.

The cross sections $\sigma_{e,x}(E_0)$ and yields $Y_{e,x}(E_0)$ of Figs. 3–8 have been simultaneously fitted using the $E1$ and $E2$ virtual photon spectra[7,8] calculated in the distorted-wave Born approximation (DWBA) assuming a point nucleus, which implies the long wavelength limit $qR \to 0$. We have tried to compensate for the failure of the long wavelength approximation by making a correction to the virtual photon spectra. This correction consists in multiplying $N^{\lambda L}(E_0,E,Z)$ inside the integrals of Eqs. (1) and (2) by the quantity

$$F^{\lambda L}(qR) = \left[\left(\frac{E}{q} \right)^L \frac{j_L(qR)}{j_L(ER)} \right]^2_{q=q_{\rm rms}}, \qquad (3)$$

where R is the radius of the nuclear ground state and q is the momentum transfer. The way in which the rms values of q were estimated is described in Ref. 1. This size-effect correction is of the same magnitude as the one proposed by Shotter.[9] We have used both the Schiff[10] and the Davies-Bethe-Maximon[11] (DBM) bremsstrahlung cross sections for $K(E_0,E)$ in Eq. (2). The $E1$ photonuclear cross sections have been represented by coarse histograms with the bins 3–4 MeV wide below 24 MeV and much wider above; they cannot show any detailed features of the cross sections. The $E2$ strength was found in all six reactions, and is obtained in a single bin 6 MeV wide at the energy of the isoscalar $E2$ giant resonance. When $E2$ strength was also included at the energy of the isovector $E2$ resonance, the additional strength obtained was consistent with zero. The resulting histograms are shown in Figs. 3–8, where the smooth curves through the data are the best fits; they were obtained in every case by using the DBM bremsstrahlung cross section and including the size effect correction to the virtual photon spectra. The main feature of the histogram representing the $E1$ strength is, of course, the giant dipole resonance located near 20 MeV. The bump that appears systematically between 50 and 60 MeV in most of the $E1$ histograms is not real and can be made to disappear using a different choice of analysis bins.

Various options were available in the fitting program, e.g., the choice of the bremsstrahlung cross section, whether or not to include the size effect correction, and the choice of the upper limit of the integration in (1) and (2). Poorer fits were always obtained with the Schiff bremsstrahlung cross section. The fitting procedure should yield the same and the true photonuclear cross section independent of the upper limit of the integrals. The inclusion of the size effect correction improves the quality of the fits, especially as the upper limit of the integrals is increased. Table III compares the amount of $E2$ strength obtained in the analysis of the (e,p) and (e,α) data when the integrals are carried out to 50 and 100 MeV with and without the size effect correction. It is clear that the correction is needed to make the result independent of the upper limit of integration. The uncertainties are smaller if the upper limit is 100 MeV because more data are included. Even with the size effect correction the amount of $E2$ strength obtained is systematically smaller for the upper limit of 100 MeV. We believe that this trend results from an inadequacy in the correction made for the alteration of the experimental goemetry by the insertion of the radiator for incident electron energies in the range 36–60 MeV. These points appear 1–2% below the best fit when the integrals are carried out to 100 MeV. Were it not for this uncertainty, we could use the experiment to determine the transi-

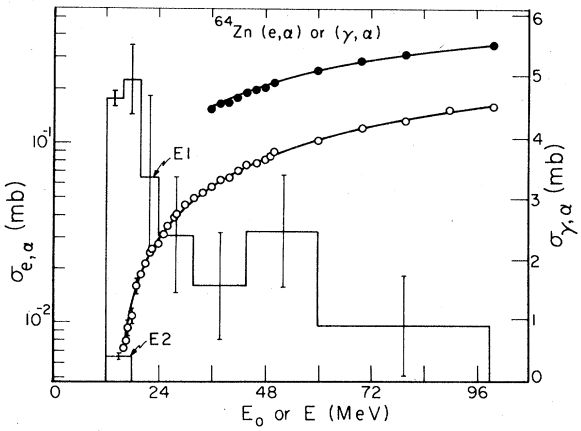

FIG. 8. The $\sigma_{e,\alpha}(E_0)$ for ^{64}Zn. See caption of Fig. 3.

TABLE III. Percentage of the $E2$ sum when only points up to 50 MeV ($E_0=50$ MeV) and when all measured points ($E_0=100$ MeV) are considered in the analysis. The bremsstrahlung cross section used is DBM. $E2$ sum: $0.22Z^2A^{-1/3}$ μb/MeV.

Nucleus	Reaction	Without size effect		With size effect	
		$E_0=50$ MeV	$E_0=100$ MeV	$E_0=50$ MeV	$E_0=100$ MeV
^{56}Fe	(e,α)	9± 3	3 ± 1	11± 3	7± 1
	(e,p)	47±30	8±11	61±32	37±15
^{59}Co	(e,α)	7± 2	4 ± 1	8± 2	5± 1
	(e,p)	32±22	4± 8	48±24	28±11
^{64}Zn	(e,α)	26± 6	12± 2	32± 6	25± 3
	(e,p)	29±43	26±15	56±46	77±21

tion charge radius required to make the magnitude of the $E2$ strength independent of the upper limit of the integration.

This experience leads us to conclude that the $E2$ strength in the α channel derived using the size effect correction and reported in Ref. 1 must be an overestimate. In that experiment the radiator was not used for electron energies above 50 MeV, whereas in the present experiment it is the data, taken with the radiator in the electron energy range 70—100 MeV, that are really limiting the derived $E2$ strength. Had the radiator been used up to 100 MeV in the previous experiment, we might also have been able to extract the $E2$ strength in the proton channel.

Table IV summarizes the amount of $E1$ and $E2$ strength found in the (e,p) and (e,α) reactions for the targets studied. The integrals have been carried out to 100 MeV and the size effect correction has been included. We show the results obtained using both the Schiff and DBM bremsstrahlung cross sections even though the latter gave a better fit and is generally accepted to be a more accurate formula because it contains Coulomb corrections and a more appropriate screening function. The large differences obtained using these two bremsstrahlung cross sections, which differ by only 10%, suggest that this kind of experiment may be a good way to determine the absolute bremsstrahlung cross section magnitude.

The $E2$ strengths in the proton and α channels of ^{64}Zn may be compared with the results of Collins *et al.*,[12] who have studied them in an (α,α',x) coincidence experiment as well as in a Hauser-Fesbach calculation. These are shown in Table V. There is agreement between the two experiments

TABLE IV. Percentage of the $E1$ and $E2$ sums in the α and proton channels. $E1$ sum: $60NZ/A$ MeV mb. $E2$ sum: $0.22Z^2A^{-1/3}$ μb/MeV. Integrals to 100 MeV.

Nucleus	Reaction	$E1$		$E2$	
		Schiff	DMB	Schiff	DBM
^{56}Fe	(e,α)	5± 1	6± 1	10± 1	7± 1
	(e,p)	67±20	82±19	82±14	37±15
	$(e,\alpha)+(e,p)$	72±20	88±19	92±14	44±15
^{59}Co	(e,α)	5± 1	7± 1	8± 1	5± 1
	(e,p)	52±10	67±12	63±10	28±11
	$(e,\alpha)+(e,p)$	57±10	74±12	71±10	33±11
^{64}Zn	(e,α)	16± 4	18± 4	33± 3	25± 3
	(e,p)	129±28	154±30	137±30	77±21
	$(e,\alpha)+(e,p)$	145±28	172±30	170±20	102±21

and the calculation for the α channel, but the $E2$ strength in the proton channel derived from the present experiment is excessive even though the error is large. On the other hand, since the total $E2$ strength excited in the (α,α') experiment of Lui *et al.*[13] is only $(38\pm10)\%$ of an energy weighted sum, the absolute magnitude obtained in the hadron and electron scattering experiments apparently differ.

Table VI shows the photonuclear cross sections derived in the present experiment integrated to 30 MeV along with (γ,n) cross sections obtained using real photons.[14,15] Summing these three integrated cross sections, we obtain 1.2—1.3 dipole sums, the same as was obtained for the nickel isotopes.[1] To achieve this result it was necessary to note that the extraordinarily large (γ,pn) cross section for ^{64}Zn is included in both the proton and neutron yield experiments. In Table VI it has been removed from the neutron channel by multiplying the integrated neutron yield cross section by 0.77, the branching ratio obtained by activation.[16]

The nucleus ^{64}Zn is a profuse emitter of protons and α particles, owing to their low binding energies. A glance at the cross sections integrated to 100 MeV given in Table IV reveals that the proton and α yields are approximately twice as great for ^{64}Zn as for the other two targets studied. This result suggests that the cross sections $\sigma(e,p\alpha)$ and $\sigma(e,2p)$, which would be counted twice in this experiment, may be very important for ^{64}Zn.

In a similar experiment Tsubota *et al.*[17] have studied the (e,p) cross section in ^{59}Co and derived an electric dipole (γ,p) cross section integrated to 29 MeV of 353 ± 25 MeV mb, 38% greater than the result shown in Table VI. This discrepancy is too large to be attributed to their use of the plane wave rather than the DWBA virtual photon spectrum. The determination of our absolute magnitudes is discussed in Ref. 1.

To get an estimate of the total photonuclear cross sections integrated to 100 MeV, we can add the integrated (γ,n) cross sections of Table VI to the derived integrated $(\gamma,p)+(\gamma,\alpha)$ cross sections of Table IV. We are omitting the $E2$ strength which is negligible when measured in MeV mb, and the quoted results were obtained using the DBM bremsstrahlung cross section. The results are 1.76 ± 0.19, 1.75 ± 0.12, and 2.36 ± 0.30 $E1$ sums for ^{56}Fe, ^{59}Co, and ^{64}Zn, respectively. These sums do not include the (γ,n) cross sections integrated between 30 and 100 MeV. The integrated cross sections for ^{56}Fe and ^{59}Co may be compared with the results obtained by Ahrens *et al.*[18] for the light elements and by Lepretre *et al.*[19] for Pb, both of whom obtain similar magnitudes. The larger integrated cross section of ^{64}Zn may result from multiple particle emission.

IV. THE ANGULAR DISTRIBUTIONS

In a related paper,[6] detailed angular distributions were reported of the α particles emitted by ^{56}Fe when irradiated by 35 MeV electrons. It was found that the α particles on the low side of the spectrum were peaked backward and those on the high side were forward of 90°. This phenomenon was explained as resulting from the interference of an $E2$ resonance near 18 MeV superimposed on an $E1$ continuum.

Because the $E2$ virtual photon spectrum rises so much more steeply toward low energies than does the $E1$ with increasing electron energy, these asymmetries should also change rapidly with electron energy. To explore this point we measured for two energy intervals at the peaks of the proton and α spectra the cross sections at the angles 62° and 118° for electron energies 20—50 MeV. The angle between the target and the beam was the same for both so that the corrections for particle energy loss in the target would be the same. The ratio $\sigma(62°)/\sigma(118°)$ as a function of incident electron energy is shown for protons in Fig. 9 and for α particles in Fig. 10. Qualitatively, there is no dramatic change in this ratio for either particle as the electron energy is changed. The 4.7 MeV protons in the peak of their spectrum are symmetric

TABLE V. Decay branches for ^{64}Zn.

Channel	Collins *et al.* (Ref. 12)	This experiment sum-rule depletion (%)	Calculation (Ref. 12)
α	20 ± 4	25 ± 3	26
p	38 ± 7	77 ± 21	46
n	59 ± 27		28

TABLE VI. $E1$ strength integrated up to 30 MeV.

Nucleus	$\int_0^{30} \sigma_{\gamma,x}(E)dE$ (MeV mb)				Fraction
	α	p	n	Total	of $E1$ sum
^{56}Fe	18± 3	256±26	735[a]	1009	1.21
^{59}Co	15± 2	211±22	884[b]	1110	1.26
^{64}Zn	66±14	545±75	616[b]	1227	1.28

[a]Reference 13.
[b]Reference 14.

about 90°, and the 8 MeV protons in the tail of the distribution are always forward peaked. The 4.5 MeV α particles are peaked backward of 90° as reported in Ref. 5. The α particles in the peak of the energy distribution are symmetric about 90°, whereas those having energies on the high energy side of the spectrum are peaked forward.

We would like to present an alternative explanation of this phenomenon. These observations have been made in the laboratory system and should be transformed into the center of mass system. To estimate the magnitude of the kinematic effects we assume that the virtual photon is absorbed at 20 MeV and that the momentum transfer is in the forward direction. Neglecting $V_{\text{c.m.}}{}^2$, the relationship between the center-of-mass and laboratory kinetic energies is

$$T_{\text{c.m.}} = T_{\text{lab}}\left[1 - \frac{2V_{\text{c.m.}}}{V_{\text{lab}}}\cos\theta\right], \tag{4}$$

where $V_{\text{c.m.}}$ is the velocity of the center of mass and V_{lab} is the particle velocity in the laboratory. The 4.7 MeV protons from ^{56}Fe observed in the laboratory correspond to 4.684 and 4.716 MeV protons emitted, respectively, at 62° and 118° in the center-of-mass system. Since these energies are all

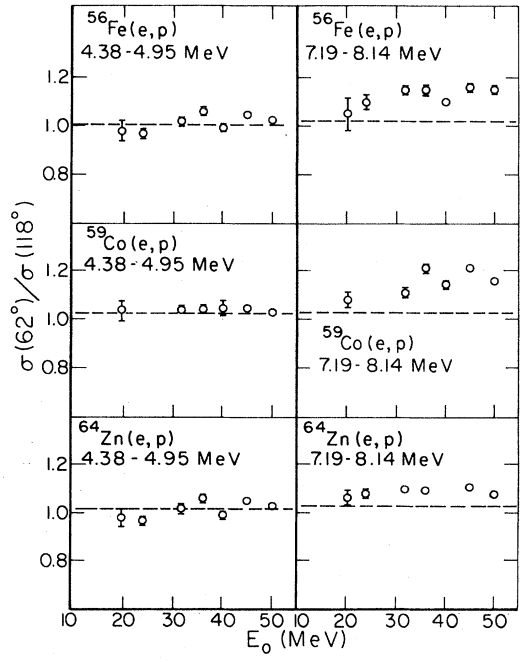

FIG. 9. The ratios of the number of protons observed in the indicated energy bite ΔT_p at 62° to the same number observed at 118°, $\sigma(62°)/\sigma(118°)$, as a function of incident electron energy.

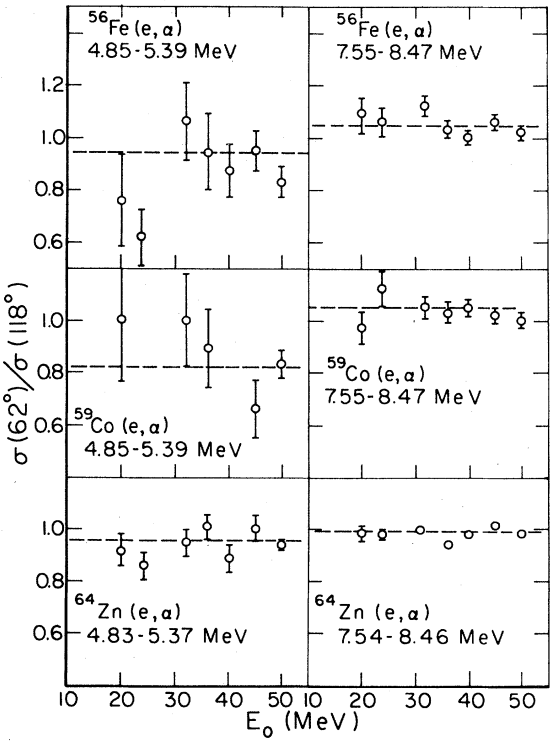

FIG. 10. The ratios of the number of α particles observed in the indicated energy bite ΔT_α at 62° to the same number observed at 118°, $\sigma(62°)/\sigma(118°)$, as a function of incident electron energy.

in the peak of the spectrum (see Fig. 1) the laboratory and center-of-mass cross sections are basically the same. The situation is, however, quite different for the 5.1 MeV α particles, because they come from a region of the spectrum (see Fig. 2) where the cross section is changing very rapidly. In the center-of-mass system they have 5.066 MeV at 62° and 5.134 MeV at 118°. The difference in the cross section at these two energies is enough to produce the observed forward-backward asymmetry. This kinematic correction removes most but not all of the asymmetry reported in Ref. 6. The dashed lines in Figs. 9 and 10 represent the kinematic correction that should be applied to our data; i.e., the measured ratios should be divided by this number. Our conclusion is that the angular distribution in the center-of-mass system is symmetric about 90° throughout most of the spectrum. The kinematic correction is, however, not enough to remove the forward peaking in the high energy tail for either protons or α particles.

V. CONCLUSIONS

The cross sections for emission of protons and alpha particles by absorption of real and virtual photons in ^{56}Fe, ^{59}Co, and ^{64}Zn have been measured. The $E1$ and $E2$ photonuclear cross sections from threshold to 100 MeV have been derived from these data. Including the neutron channel, the $E1$ strength integrated to 100 MeV amounts to nearly 2 $E1$ sums as has already been observed for other elements in the total cross section measurements. The $E2$ strength observed in the proton and α channels for the three targets appear to depend only on the binding energies and the Coulomb barrier height. The angular distributions of both protons and alpha particles are symmetric about 90° in the center-of-mass system, except for the high energy tails, which are always forward peaked. In fitting the data it became apparent that a size effect correction was necessary above $\sim$50 MeV incident electron energy and that the one used has the correct dependence on momentum transfer.

ACKNOWLEDGMENTS

The authors wish to acknowledge the joint support of Conselho Nacional de Desenvolvimento Cientifico e Technologico (Brazil) and the National Science Foundation, which has allowed them to collaborate on this project. One of us (R. G. L.) was supported by the Deutsche Forschungsgemeinschaft (West Germany) during his tenure at the National Bureau of Standards. The authors also wish to thank Dr. Louis Wright for supplying the detailed DWBA virtual photon spectra that made the analysis possible.

---

*On leave from the Max-Planck-Institute für Chemi, Mainz, Germany.

†On leave from the university of Sao Paulo, Sau Paulo, Brazil.

[1]E. Wolynec, W. R. Dodge, R. G. Leicht, and E. Hayward, Phys. Rev. C 22, 1012 (1980).

[2]E. Hayward, in *Giant Multipole Resonances,* edited by F. E. Bertrand (Harwood, New York, 1980).

[3]A. G. Flowers, D. Branford, J. C. McGeorge, A. C. Shotter, P. Thorley, and C. H. Zimmerman, Phys. Rev. Lett. 43, 323 (1979).

[4]T. Urano, M. Hirooka, and M. Sugawara, in *Proceedings of the International Conference on Nuclear Physics with Electromagnetic Interactions, Mainz, 1979* (Springer, Berlin, 1979).

[5]K. Shoda, K. Abe, T. Ishizuka, N. Kawamura, M. Oyamada, and Baik-Nung Sung, J. Phys. Soc. Jpn. 25, 664 (1968).

[6]D. M. Skopik, J. Asai, and J. J. Murphy II, Phys. Rev. C 21, 1746 (1980).

[7]W. W. Gargaro and D. S. Onley, Phys. Rev. C 4, 1032 (1971).

[8]C. W. Soto Vargas, D. S. Onley, and L. E. Wright, Nucl. Phys. A288, 45 (1977).

[9]A. C. Shotter, J. Phys. G 5, 371 (1979).

[10]L. I. Schiff, Phys. Rev. 83, 252 (1951).

[11]J. L. Mathews and R. O. Owens, Nucl. Instrum. Methods 111, 157 (1973).

[12]M. T. Collins, C. C. Chang, S. L. Tabor, Phys. Rev. C 24, 387 (1981).

[13]Y. -W., Lui, P. Bogucki, J. D. Bronson, U. Garg, C. M. Rozsa, and D. H. Youngblood, Phys. Lett. 93B, 31 (1980).

[14]S. Costa, F. Ferrero, S. Ferroni, C. Molino and R. Malvano, Phys. Lett. 11, 324 (1964).

[15]B. L. Berman and S. C. Fultz, Rev. Mod. Phys. 47, 713 (1975).

[16]C. Yamaguchi, J. Phys. Soc. Jpn. 34, 1123 (1973).

[17]H. Tsubotu, S. OiKawa, J. Uegaki, and T. Tamae, Nucl. Phys. A303, 333 (1978).

[18]J. Ahrens, H. Borchert, K. H. Czock, H. B. Eppler, H. Gimm, H. Gundrum, M. Kronig, P. Riehn, G. Sita Ram, A. Zieger, and B. Ziegler, Nucl. Phys. A251, 479 (1975).

[19]A. Lepretre, H. Beil, R. Bergere, P. Carlos, J. Fagot, A. Vessiere, J. Ahrens, P. Axel, and U. Kneissl, Phys. Lett. 79B, 43 (1978).